

This article was downloaded by: [Moskow State Univ Bibliote]

On: 15 April 2012, At: 12:58

Publisher: Taylor & Francis

Informa Ltd Registered in England and Wales Registered Number: 1072954 Registered office: Mortimer House, 37-41 Mortimer Street, London W1T 3JH, UK



Molecular Crystals and Liquid Crystals

Publication details, including instructions for authors and subscription information:

<http://www.tandfonline.com/loi/gmcl20>

Optical Shuttering and Filtering Action in Nematogens of Supra Molecular Hydrogen-Bonded Liquid Crystals

N. Pongali Sathya Prabu^a & M. L. N. Madhu Mohan^a

^a Liquid Crystal Research Laboratory (LCRL), Bannari Amman Institute of Technology, Sathyamangalam, India

Available online: 20 Mar 2012

To cite this article: N. Pongali Sathya Prabu & M. L. N. Madhu Mohan (2012): Optical Shuttering and Filtering Action in Nematogens of Supra Molecular Hydrogen-Bonded Liquid Crystals, *Molecular Crystals and Liquid Crystals*, 557:1, 190-205

To link to this article: <http://dx.doi.org/10.1080/15421406.2011.648059>

PLEASE SCROLL DOWN FOR ARTICLE

Full terms and conditions of use: <http://www.tandfonline.com/page/terms-and-conditions>

This article may be used for research, teaching, and private study purposes. Any substantial or systematic reproduction, redistribution, reselling, loan, sub-licensing, systematic supply, or distribution in any form to anyone is expressly forbidden.

The publisher does not give any warranty express or implied or make any representation that the contents will be complete or accurate or up to date. The accuracy of any instructions, formulae, and drug doses should be independently verified with primary sources. The publisher shall not be liable for any loss, actions, claims, proceedings, demand, or costs or damages whatsoever or howsoever caused arising directly or indirectly in connection with or arising out of the use of this material.

Optical Shuttering and Filtering Action in Nematogens of Supra Molecular Hydrogen-Bonded Liquid Crystals

N. PONGALI SATHYA PRABU
AND M. L. N. MADHU MOHAN*

Liquid Crystal Research Laboratory (LCRL), Bannari Amman Institute
of Technology, Sathyamangalam, India

A novel series of linear supra molecular hydrogen-bonded liquid crystals (SMHBLC) have been isolated. Complimentary hydrogen bonds are formed between various alkyloxy benzoic acids. The formation of hydrogen bond is conformed by FTIR studies. This series exhibits rich phase variance as evinced by various textures through polarizing optical microscopic (POM) studies. Differential scanning calorimetry (DSC) studies revealed that the transition temperatures and corresponding enthalpy values are elucidated from the DSC thermograms. Phase diagram has been constructed through POM and DSC data. An interesting finding is the observation of a new smectic ordering labeled as smectic X. This phase has been characterized by various techniques. Optical tilt angle in smectic C phase of various homologues has been measured and fitted to theoretical values. The critical exponent β value estimated by fitting the data of tilt angle is found to agree with the Mean Field prediction. Light filtering action of these mesogens in nematic phase has been studied. It is interesting to find that the magnitude of the cut off frequencies in higher homologues is almost similar while lower homologues behave as a band pass filter. Another unique feature is the observation of a notch filtering action in one of the homologue. Yet another interesting finding is the optical shuttering action of the mesogens in nematic phase. On application of an external field at a threshold field, these mesogens inhibits light thus behaving as optical shutters. In view of the above properties, these mesogens can be exploited for commercial applications.

Keywords Light filtering action; optical shuttering; smectic X; supra molecular hydrogen-bonded liquid crystals

1. Introduction

Liquid crystals possess anisotropic properties and are recognized as new dynamic functional molecular materials with wide area of application in the display device sector. Among the different types of liquid crystals existing, thermotropic liquid crystals form an elite class. Many groups are working on hydrogen-bonded liquid crystals (HBLC) due to abundant availability of various acceptor and donor functional groups and versatility for commercial applications [1–12]. Hydrogen bond, the fifth type of interaction existing between the chemical components, takes part actively in the synthesis, and is considered to be the

*Address correspondence to M. L. N. Madhu Mohan, Liquid Crystal Research Laboratory (LCRL), Bannari Amman Institute of Technology, Sathyamangalam 638 401, India. Tel: +91 9442437480; Fax: +91 4295 223775. E-mail: mln.madhu@gmail.com

basis for the origin of new stable mesophases with a wide thermal stability [4]. The first ever hydrogen-bonded liquid crystalline material is resulted from the dimerization of aromatic p-n alkyloxy carboxylic acids. Hydrogen bonds having lower bonding and activation energies showed a profound influence on their thermal properties, viz., melting points, enthalpies of vaporization, and mesomorphic phase behavior [11]. There are reports [13] in the literature that to obtain mesogenic hydrogen-bonded liquid crystals, it is enough if one of the compounds exhibits mesogenic properties. It is surprising to note that mesogens exhibiting liquid crystalline phases can also be formed through two nonmesogenic compounds [14–16].

HBLC nematogens exhibit optical shuttering action [17, 18] and light-modulating applications [19]. Design, synthesis, and characterization of supra molecular hydrogen-bonded liquid crystals (SMHBLC) materials which can be used for applicational purposes is a challenging task. Alkyloxy benzoic acids are mesogenic in nature and form complimentary hydrogen bonds with any aliphatic acids giving rise to HBLC. It is reported [18–31] that when any mesogenic/nonmesogenic moiety is interacted with alkyloxy benzoic acid, HBLC are formed with single, double, and multiple hydrogen bonds. These hydrogen-bonded materials can be used for applications only if it possesses a phase that can be tuned by an external stimulus like an electric or thermal field. The design of the molecular structure helps in a proper molecular alignment of the phase, which plays a pivotal role in ascertaining the extent of utility of the mesogen. With our previous experience [17–28] in synthesis and characterizing of various types of liquid crystals and with the above aims, a novel series of hydrogen-bonded mesogens are synthesized. Light modulation, filtering action, and optical shuttering action can be realized with proper design of the mesogens.

The central theme of the aimed research work involves in design, synthesis, and characterization of eight homologous series of SMHBLC formed between p-n-alkyloxy benzoic acid (nBAO) and p-n-alkyloxy benzoic acids (mBAO) referred as nBAO + mBAO, where m varies from 5 to 12. These eight series can be referred as 5BAO + mBAO, 6BAO + mBAO, 7BAO + mBAO, 8BAO + mBAO, 9BAO + mBAO, 10BAO + mBAO, 11BAO + mBAO, and 12BAO + mBAO that give rise to 56 different hydrogen-bonded complexes. In this paper, systematic study of the mesogenic properties exhibited by seven complexes of 12BAO + mBAO homologous series are discussed.

2. Experimental

Optical textural observations are made with a Nikon polarizing microscope equipped with Nikon digital CCD camera system with five mega pixels and 2560×1920 pixel resolutions. The liquid crystalline textures are processed, analyzed, and stored with the aid of ACT-2U imaging software system. The temperature control of the liquid crystal cell is equipped with Instec HCS402-STC 200 temperature controller (Instec, USA) to a temperature resolution of $\pm 0.1^\circ\text{C}$. This unit is interfaced to computer by IEEE – STC 200 to control and monitor the temperature. The transition temperatures and corresponding enthalpy values are obtained by differential scanning calorimetry (DSC) (Shimadzu DSC-60, Japan). FTIR spectra is recorded (ABB FTIR MB3000) and analyzed with the MB3000 software. Liquid crystalline sample is taken to its isotropic state and filled in four micrometer commercially available (Instec Research Instrumentation Technology, Colorado, USA) polyimide coated homogeneous aligned antiparallel cell. Silver leads are taken for contact and is connected

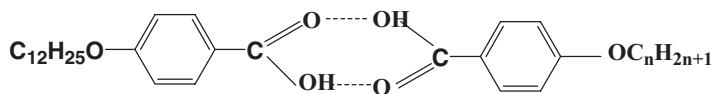


Figure 1. Molecular structure of 12BAO + mBAO homologous series.

to the Agilent 4192A LF Impedance Analyzer. The p-n-alkyloxy benzoic acids are supplied by Sigma Aldrich, (Germany) and all the solvents used are HPLC grade.

2.1 Synthesis of HBLC

Intermolecular hydrogen-bonded mesogens are synthesized by the addition of one mole of dodecyloxy benzoic acid (12BAO) with one mole of p-n alkyloxy benzoic acids (nBAO, where n represents pentyloxy to undecyloxy benzoic acid) in N, N-Dimethyl formamide (DMF). Further, they are subjected to constant stirring for 12 hours at ambient temperature of 30°C till a white precipitate in a dense solution is formed. The white crystalline crude complexes so obtained by removing excess DMF are then recrystallized with dimethyl Sulfoxide (DMSO). The molecular structure of the present homologous series of dodecyloxy benzoic acid with p-n- alkyloxy benzoic acids (12BAO + mBAO) is shown in Fig. 1, where m represents the alkyloxy carbon number.

3. Results and Discussion

Hydrogen-bonded complexes isolated under the present investigation mostly are white crystalline solids and are stable at room temperature (30°C). They are insoluble in water and sparingly soluble in common organic solvents such as methanol, ethanol, and benzene and dichloromethane. However, they show a high degree of solubility in coordinating solvents like DMSO, DMF and pyridine. All these mesogens melt at specific temperatures ~86.2°C (Table 1). They show high thermal and chemical stability when subjected to repeated thermal scans performed during polarizing optical microscopic (POM) and DSC studies.

3.1 Phase Identification

The observed phase variants, transition temperatures, and corresponding enthalpy values obtained by DSC in cooling and heating cycles for the 12BAO + mBAO series is presented in Table 1.

3.1.1 12BAO + mBAO Homologous Series. The mesogens of the dodecyloxy benzoic acid and p-n-alkyloxy benzoic acids homologous series (12BAO + mBAO) are found to exhibit characteristic textures [32], viz., nematic (threaded texture, Plate 1), smectic X (worm like texture, Plate 2), smectic C (broken focal conic texture, Plate 3) and smectic F (chequered board texture, Plate 4) respectively. The phase sequence of 12BAO + mBAO series obtained by POM and DSC studies can be represented as below:

Isotropic \Rightarrow N \rightarrow Sm C \Rightarrow Crystal (12BAO + 5BAO and 6BAO)

Isotropic \Rightarrow N \rightarrow Sm C \Rightarrow Sm F \Rightarrow Crystal (12BAO + 7BAO)

Isotropic \Rightarrow N \rightarrow Sm X \Rightarrow Sm C \Rightarrow Crystal (12BAO + mBAO, where n = 8 to 11)

Single and double arrow indicates monotropic and enantiotropic transitions.

Table 1. Transition temperatures obtained by different techniques

Carbon number	Phase variance	Techniques	Crystal to melt	N	X	C	F	Crystal
5	NC	DSC (h)	70.4 (45.19)	139.1 (7.84)		#		
		DSC (c)		135.3 (7.17)		83.4 (0.96)		63.0 (44.82)
		POM (c)		135.9		83.8		63.2
6	NC	DSC (h)	68.6 (26.97)	141.4 (5.12)		#		
		DSC (c)		138.1 (5.50)		109.2 (1.15)		62.0 (26.43)
		POM (c)		138.9		109.9		62.5
7	NCF	DSC (h)	70.6 (27.96)	139.6 (4.79)		#	111.8 (2.41)	
		DSC (c)		135.6 (5.16)		119.1 (0.32)	109.2 (2.29)	58.5 (28.82)
		POM (c)		136.3		119.6	109.6	59.7
8	NXC	DSC (h)	73.1 (23.35)	139.3 (3.24)				
		DSC (c)		133.6 (6.3)	#	116.3 (2.65)		61.2 (26.96)
		POM (c)		134.3	117.7	116.8		61.4
9	NXC	DSC (h)	68.5 (21.05)	137.8 (4.26)	#	125.1 (5.16)		
		DSC (c)		133.3 (4.26)	#	122.4 (4.86)		64.4 (17.64)
		POM (c)		133.9	125.7	122.8		64.6
10	NXC	DSC (h)	77.9 (43.16)	140.0 (7.58)	#	127.9 (5.10)		
		DSC (c)		135.5 (7.63)	#	124.5 (4.55)		72.3 (31.25)
		POM (c)		136.2	125.6	124.9		72.5
11	NXC	DSC (h)	86.2 (26.18)	139.1 (4.97)	#	131.3 (7.67)		
		DSC (c)		135.1 (7.25)	#	127.8 (5.42)		80.7 (33.82)
		POM (c)		135.8	127.3	128.4		80.8

Note: (h), heating run; (c), cooling run; ΔH in J/g is given in parentheses; #, not resolved.

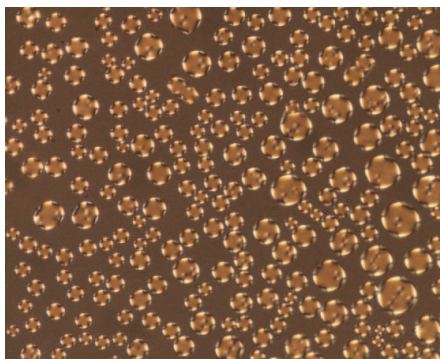


Plate 1. Thread-like texture of nematic.



Plate 2. Worm-like texture of smectic X.

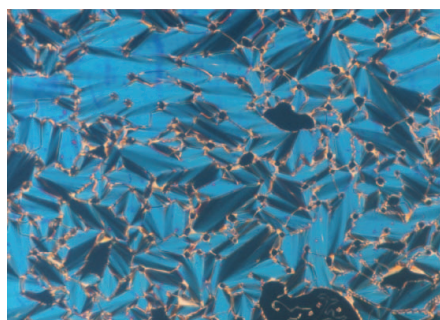


Plate 3. Broken focal conic texture of smectic C.

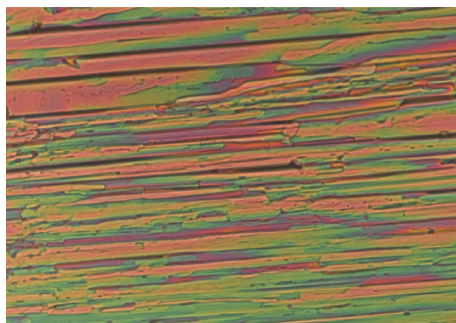


Plate 4. Checkered board texture of smectic F.

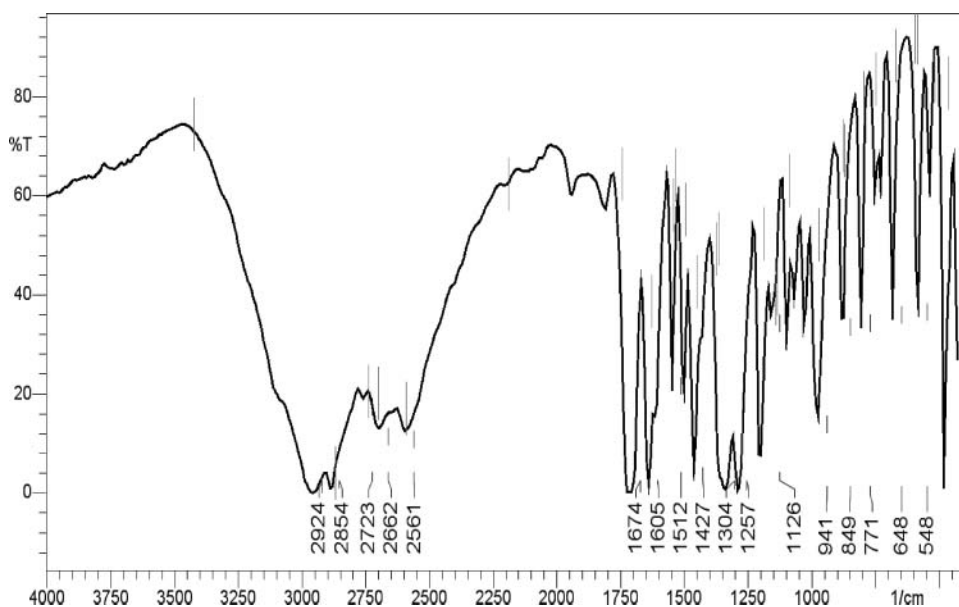


Figure 2. FTIR spectra of 12BAO + 11BAO complex.

3.2 Fourier Transform Infrared Spectroscopy (FTIR)

IR spectra for all the seven homologues of 12BAO + mBAO series have been recorded in the solid state (KBr) at room temperature. As a representative case, FTIR spectrum of 12BAO + 11BAO complex is shown in Fig. 2 and is discussed elaborately. It is reported [33, 34] that in the alkyloxy benzoic acids, carboxylic acid exists in monomeric form, and the stretching vibration of C=O is observed at 1760 cm^{-1} . Further, it is known [34] that when a hydrogen bond is formed between carboxylic acids it results in lowering of the carbonyl frequency, which has been detected in the present hydrogen-bonded complexes. A noteworthy feature in the spectrum of the 12BAO + 11BAO is the appearance of sharp peak at 1674 cm^{-1} , which clearly suggests the dimer formation in particular the carbonyl group vibration. [35–37]. A carboxylic acid existing in monomeric form in dilute solution absorbs at about 1760 cm^{-1} because of the electron withdrawing effect. However, acids in concentration solution or in solid state tend to dimerize through hydrogen bonding. It is reported [34] that this dimerization weakens the C=O bond and lowers the stretching force constant K , resulting in a lowering of the carbonyl frequency of saturated acids to $\sim 1710\text{ cm}^{-1}$. This result concurs with the reported data of Kato et al. [33]. Hence, in the present complexes the formation of H bonding is established by FTIR. A similar trend of result is followed in all the synthesized hydrogen-bonded complexes.

3.3 DSC Studies

DSC thermograms are obtained in heating and cooling cycle. The sample in the crimped aluminum cell is heated with a scan rate of $10^\circ\text{C}/\text{min}$ and held at its isotropic temperature for two minutes so as to attain thermal stability. The cooling run is performed with a programmed scan rate of $10^\circ\text{C}/\text{min}$. The respective equilibrium transition temperatures and corresponding enthalpy values of the various homologues are listed in Table 1. These DSC

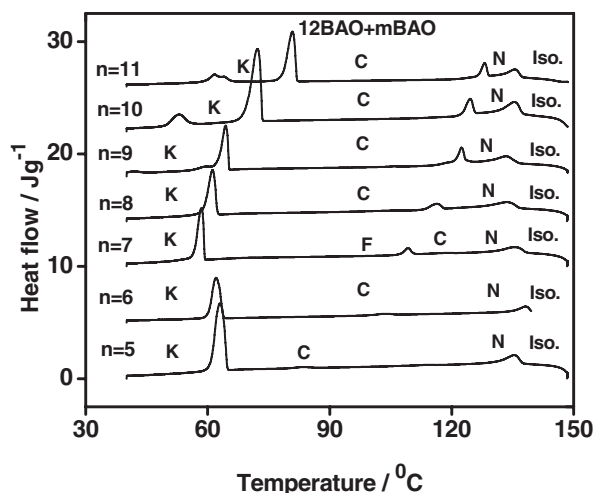


Figure 3. DSC exothermic thermograms for all homologues.

results concur with the POM data. The DSC exothermic curves of all the complexes have been depicted in Fig 3.

3.4 Phase Diagram of Pure *p*-*n*-Alkyloxy Benzoic Acids

The phase diagram of pure *p*-*n*-alkyloxy benzoic acid is reported [38] to compose of two phases namely, nematic and smectic C.

3.4.1 Phase Diagram of 12BAO + mBAO. Figure 4 illustrates the phase diagram of 12BAO + mBAO homologous series. Following conclusions can be made from the phase diagram.

- i) Phase diagram consists of four phases, viz. nematic, smectic X, smectic C, and smectic F.
- ii) Thermal phase width of nematic is larger in lower homologous compounds compared to the higher counter parts.
- iii) Four compounds (12BAO + 8BAO, 12BAO + 9BAO, 12BAO + 10BAO, and 12BAO + 11BAO) exhibiting smectic X phase with varying thermal ranges.
- iv) smectic F, the highly ordered phase is observed only in the 12BAO + 7BAO complex with large thermal span.

4. Optical Tilt Angle Measurements in Smectic C

The optical tilt angle has been experimentally measured by optical extinction method [39] in smectic C phase of all the members of the 12BAO + mBAO homologous series. Figure 5 depicts such variation of optical tilt angle with temperature for various members of 12BAO + mBAO (where $n = 5$ to 11) series respectively. In Fig. 5, the theoretical fit obtained from the Mean Field theory is denoted by a solid line. The magnitude of the tilt angle increases with decreasing temperature and attains a saturation value. The high magnitudes of the tilt angle are attributed to the direction of the soft covalent hydrogen bond interaction which spreads along molecular long axis with finite inclination [40].

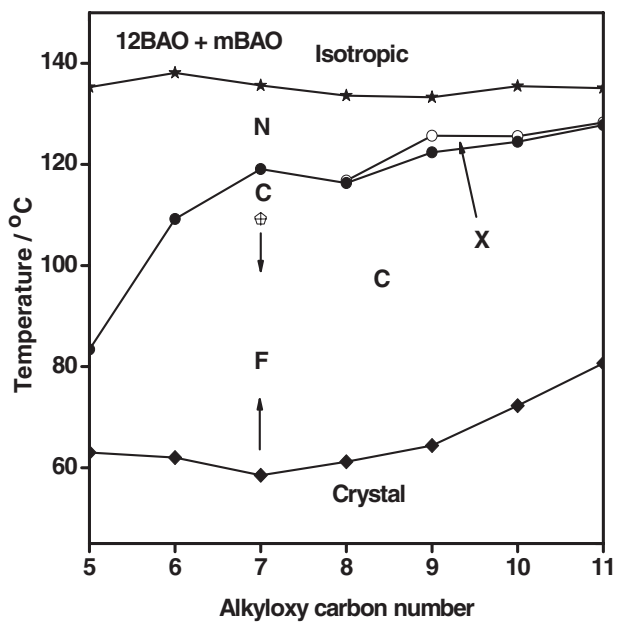


Figure 4. Phase diagram of 12BAO + mBAO series.

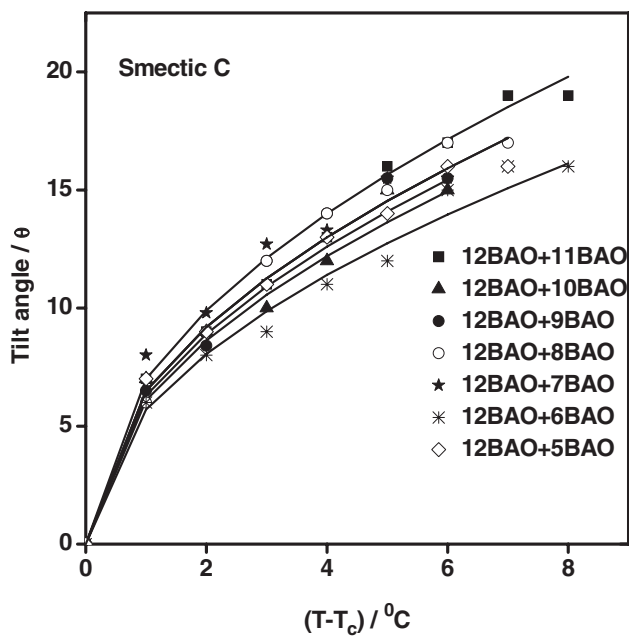


Figure 5. Temperature variation of tilt angle in smectic C phase for 12BAO + mBA series. Solid line denotes the fit.

Tilt angle is a primary order parameter [39] and the temperature variation is estimated by fitting the observed data of $\theta(T)$ to the relation

$$\theta(T) \propto (T_C - T)^\beta \quad (1)$$

The critical exponent β value estimated by fitting the data of $\theta(T)$ to the above Eq. (1) is found to be 0.50 to agree with the Mean Field prediction [41, 42]. The solid lines in the Fig. 5 depict the fitted data for various mesogens. Further, the agreement of magnitude of $\beta(0.5)$ with Mean Field value (0.5) infers the long-range interaction of transverse dipole moment for the stabilization of tilted smectic C phase.

5. Characterization of Smectic X Phase

In the higher homologues, viz., 12BAO + 8BAO, 12BAO + 9BAO, 12BAO + 10BAO, and 12BAO + 11BAO, a new phase named as smectic X phase has been observed. We had characterized this phase in our previous results [23, 43, 44] in various other HBLC systems. This phase is sandwiched between nematic and traditional smectic C. The optical morphology of this phase is a worm-like texture and is shown as Plate 2. The thermal phase width of smectic X varied from 0.7°C to 2.9°C in various homologues. The presence of the helix, which is detected by the optical studies, and the tilt angle measurements in this phase confirms it to be a new smectic ordering.

5.1 Textural Observations of Smectic X

On slow cooling from nematic phase at a rate of 0.1°C/min a new phase labeled as smectic X is observed. The darker part of the worm and its opposite handed is clearly visualized in Plate 2, which determines the phase to be tilted. This evidence supports it to be a titled phase. Furthermore, the variation of the optical tilt angle with temperature is another strong evidence for this ordering to be smectic. This phase stabilizes as the temperature is further decreased and the corresponding fully grown smectic X phase texture is shown in Plate 2. The worms are curved and are observed through out the liquid crystal cell. In fact, they act as the grating elements, which manifest the helicoidal structure of this phase. The observation of diffraction first and second order pattern in this phase is a token of evidence for the presence of helicoidal structure. In the entire thermal span of this phase, neither the size (diameter) nor the length of the worms is altered. On further decrement of temperature, broken focal conic texture of smectic C (Plate 3) is observed. These results are in concurrence with our previous reported data.

5.2 Thermodynamics of Smectic X

The smectic X phase is observed over a very narrow thermal span. The nematic to smectic X phase transition is second order as it is not resolved in DSC thermograms even at a very low scan rate of 1°C/min. On the other hand, in all the higher order homologues exhibiting smectic X phase, the phase transition from smectic X to smectic C is first order transition with considerable enthalpy values as given in Table 1. Figure 3 depicts the exothermic DSC traces for various homologues, which also includes isotropic to nematic and smectic X to smectic C transition. Furthermore, the nematic to smectic X phase transition, which is not resolved in DSC, is clearly resolved in POM experiment both in the heating and cooling cycle, which indicates the transition to be enantiotropic.

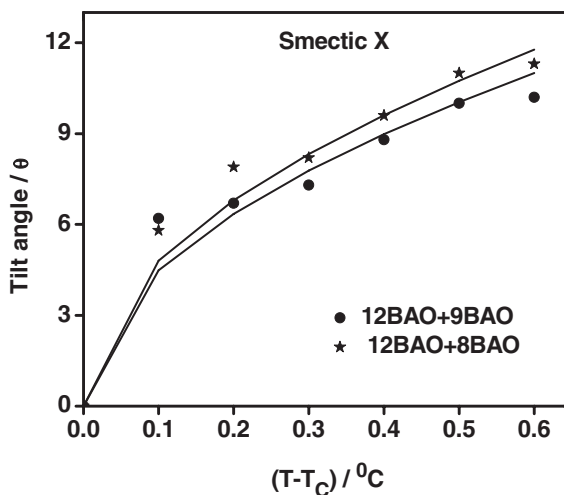


Figure 6. Temperature variation of tilt angle in smectic X phase for 12BAO + 8BAO and 12BAO + 9BAO complexes.

5.3 Optical Tilt Angle Measurements in Smectic X

Optical tilt angle in smectic X phase of various complexes has been measured. As a representative case, the tilt angle in 12BAO + 8BAO and 12BAO + 9BAO is plotted in Fig. 6, the theoretical values are shown as solid line. The critical exponent β value estimated by fitting the data of $\theta(T)$ to the Eq. (1) is found to be 0.50 to agree with the Mean Field prediction [41, 42]. The magnitude of the tilt angle increases with decrease of temperature. The saturated magnitude of the tilt angle in 12BAO + 8BAO and 12BAO + 9BAO complexes is $\sim 12^\circ$. This magnitude of tilt angle is considerably less compared to its value for the same complexes in its corresponding smectic C phase.

5.4 Helicoidal Structure in Smectic X

In the present work, the helical pitch is measured using a He–Ne red laser light on the liquid crystal sample filled in a commercially available buffed conducting cell. The details of the experimental set up are reported [23] elsewhere. The first and second order diffraction patterns are observed, which confirms the presence of the helicoidal structure in smectic X phase. The magnitude of the helix in 12BAO + 8BAO and 12BAO + 9BAO complexes is observed to be $\sim 20 \mu$. At the smectic X to smectic C transition, the sharp diffraction pattern diffuses indicating the phase transition.

6. Optical Shuttering Action

From our previous work [18, 25, 45] on HBLC, we observe that when a threshold magnitude of field (at both the bias) is applied to the LC cell in nematic phase, the shuttering action takes place, i.e., the percentage of transmitted light becomes extinct in the conducting area, which is clearly noted from the texture given (Plate 5) while the texture is unaltered in the nonconducting area of the LC cell. This extinction of transmitted light from the LC cell is referred as optical shuttering action and is purely based on the molecular alignment with respect to the applied field. Thus, the physical mechanism is the orientation of the

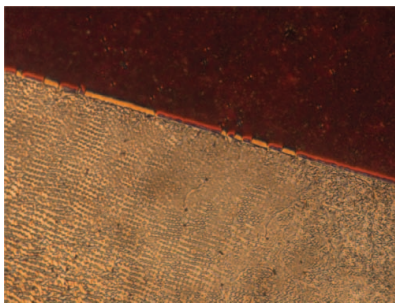


Plate 5. Optical shuttering action observed in 12BAO + 6BAO complex.

dielectrically reoriented domains. In off state, the domains allow the light to pass while in on state the light is inhibited.

The present complexes, viz., 12BAO + nBAO ($n = 6, 8$, and 11) when subjected to various strengths of external dc bias voltage, optical shuttering action is observed. In the entire thermal span of nematic phase, when an applied dc bias voltage (E_0) exceeds a threshold value (E_1), the emergent light from the liquid crystal is observed to be extinct, which is referred as optical shuttering action. This transition is classified as E_0 to E_1 , which is referred to as OS (Optical Shutter). As a representative case, optical shuttering action in 12BAO + 11BAO is discussed. Plate 5 depicted clearly indicates the optical shuttering action in the nematic phase with influence of applied field. From Plate 5, the optical shuttering action is observed in the conducting while nematic texture is seen in the nonconducting area. Immediately after withdrawing the bias voltage, the original texture of the nematic phase is retained. Thus, this process is reversible with applied bias voltage. In the entire thermal span of nematic phase of these complexes, this phenomenon is observed. While in the other phases succeeding nematic phase no such transition is found. Thus, the above transitions can be represented as:

$$E_0 \rightleftharpoons E_1 \text{ (Optical Shutter)} \quad (2)$$

The threshold values of all the SMHBLC are tabulated in the Table 2. These data are plotted as Fig. 7. It is remarkable to note that the threshold voltage values increase with increase in alkyloxy carbon number of the homologues. As the chain length increases the conjugation is also enhanced. The l/d ratio plays a vital role in increasing the threshold voltage.

Table 2. Threshold field values obtained for various complexes

Hydrogen-bonded complexes	Threshold values (Volts/micrometer)
12BAO + 6BAO	1.75 and -1.75 .
12BAO + 8BAO	2.0 and -2.0
12BAO + 11BAO	2.75 and -2.75 .

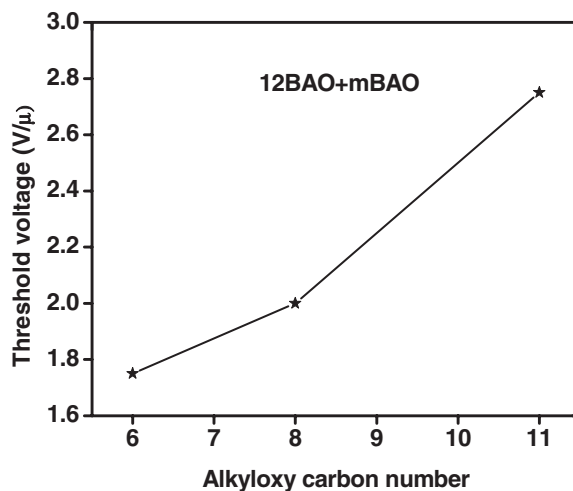


Figure 7. Variation of threshold voltage with respect to alkyloxy carbon number.

6.1 Orientation of the Domains

As a representative case, the variation of capacitance with various strengths of applied stimulus in nematic phase of 12BAO + 11BAO complex is plotted in the Fig. 8. From Fig. 8, the following points can be observed:

- i) As the voltage is increased, the magnitude of the capacitance linearly increased in both the polarities. Thus, it can be inferred that same type of molecular orientation process is occurring in both the polarities.
- ii) At the threshold magnitude of the field ($\pm 2.75 \text{ V}/\mu$) where optical shuttering occurs, the exponential behavior in the magnitude of the capacitance is noticed. This stands

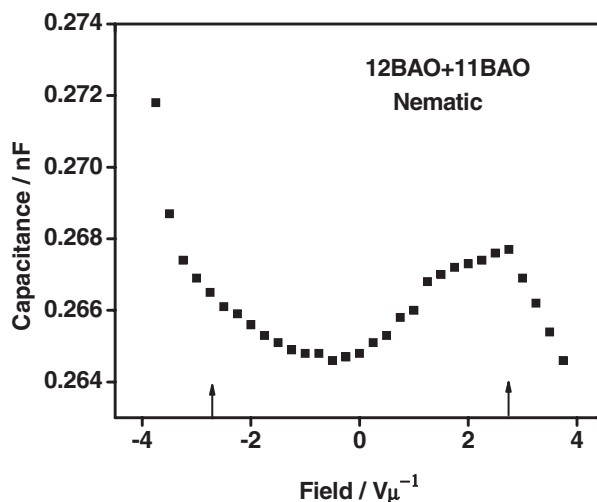


Figure 8. Light intensity profile as a function of applied stimulus for 12BAO + 11BAO complex in nematic phase.

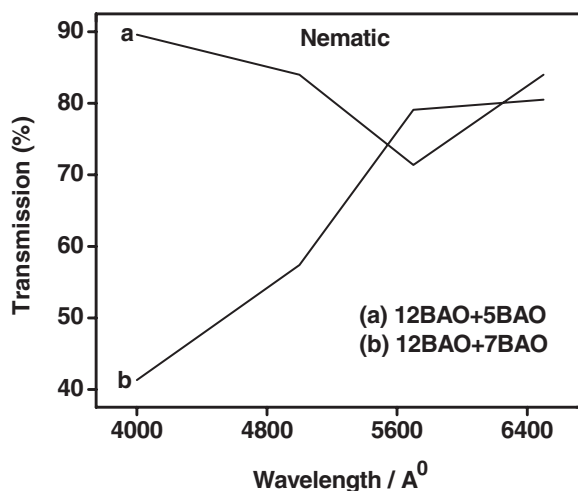


Figure 9. Filtering action in 12BAO + 5BAO and 12BAO + 7BAO complexes.

as a token of evidence that optical shuttering is induced because of the dielectrically reoriented domains.

7. Light Filtering Action

It is reported [46, 47] that nematic liquid crystal optical filters are capable of transmitting light substantially at all wavelengths while reflecting light over a single, generally narrow, and wavelength band. From the literature of nematic liquid crystals [48], it can be inferred that the unique optical properties of liquid crystal elements can be exploited to provide a wide variety of narrow band filtering functions extending over a wide wavelength range

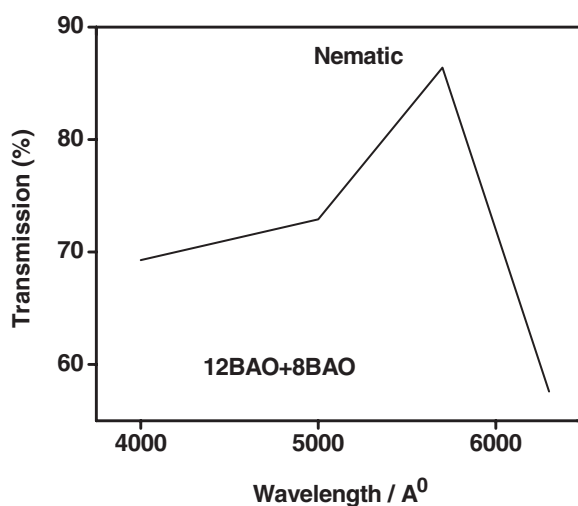


Figure 10. Filtering action in 12BAO + 8BAO complex.

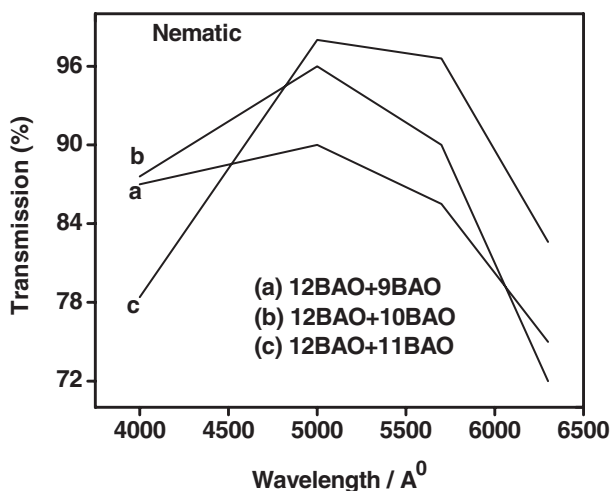


Figure 11. Filtering actions in higher order homologues.

from the near ultraviolet to the far infrared. The liquid crystal sample is filled in four micrometer commercially available polyimide coated homogeneous aligned antiparallel cell. The LC sample is mounted on circular graduated stage of polarizing microscope which is sandwiched between crossed analyzer and polarizer.

It may be recalled that the vector n representing the direction of preferred orientation of the molecules in the neighborhood of any point is termed as director. Its orientation can change continuously and in a systematic manner from point to point in the medium. So, the external forces and fields acting on the liquid crystal can result in a translational motion of the fluid as also in an orientational motion of the director. The director is parallel to the molecules and perpendicular to the transmitted light. The normalization was done with respect to the maximum percentage of light transmitted from the LC cell.

Figure 9 represents the application of 12BAO + 5BAO and 12BAO + 7BAO complexes as band pass filters while the variation of percentage polarized transmission with wavelength for the 12BAO + 8BAO complex indicates the usage of it as notch filters in its nematic phase, which is clearly portrayed in Fig. 10. From Fig. 11, it is observed that the higher homologues, viz., 12BAO + 9BAO, 12BAO + 10BAO, and 12BAO + 11BAO complexes show a similar trend of transmission of polarized light which clearly indicates that the visible region is allowed to pass, while the ultraviolet radiation is blocked. Thus, these liquid crystal complexes can be used as an effective filter for ultraviolet region of the spectrum.

Acknowledgments

Infrastructural support provided by Bannari Amman Institute of Technology and the blessings of Almighty Bannari Amman are gratefully acknowledged.

References

- [1] Kihara, H., Kato, T., Uryu, T., & Frechet, J. M. J. (1996). *Chem. Mater.*, 8, 961.
- [2] Yu, L. J. (1993). *Liq. Cryst.*, 14, 1303.

- [3] Paleos, C. M., & Tsiourvas, D. (1995). *Angew.Chem. Intl. Ed. Engl.*, 34, 1696; Paleos, C. M., & Tsiourvas, D. (2001). *Liq.Cryst.*, 28, 1127.
- [4] Xu, B., & Swager, T. (1996). *J. Shem. Soc.*, 117, 5011.
- [5] Malik, S., Dhal, P. K., & Mashelkar, R. A. (1995). *Macromolecules*, 28, 2159.
- [6] Sideratou, Z., Tsiourvas, D., Paleos, C. M., & Skoulios, A. (1997). *Liq.Cryst.*, 22, 51.
- [7] Clark, N. A., & Lagerwall, S. T. (1980). *Appl. Phys. Lett.*, 36, 899.
- [8] Lee, J., Chandani, A. D. L., Itoh, K., Ouchi, Y., Takezoe, H., & Fukuda, A. (1990). *Jap. J. Appl. Phys.*, 29, 1122.
- [9] Fukumasa, M., Kato, T., Uryu, T., & Frechet, J. M. J. (1993). *Chem. Lett.*, 22, 65.
- [10] Kato, T., Fujishima, A., & Frechet, J. M. J. (1990). *Chem. Lett.*, 22, 919.
- [11] Kumar, P. A., Srinivasulu, M., & Pisipati, V. G. K. M. (1999). *Liq.Cryst.*, 26, 1939.
- [12] Petrov, M. P., & Tsonev, L. V. (1996). *Liq.Cryst.*, 21, 543.
- [13] Tian, Y. Q., He, X., Zhao, Y. Y., Tang, X. Y., Jin Li, T., & Huang, X. M. (1998). *Mol. Cryst. Liq. Cryst.*, 309, 19.
- [14] Kang, S. K., & Samulski, E. T. (2000). *Liq. Cryst.*, 27(3), 371.
- [15] Hentrich, F., Diele, S., & Tschierske, C. (1994). *Liq. Cryst.*, 17, 827.
- [16] Kobayashi, Y., & Mtsunage, Y. (1987). *Bull. Chem. Soc. Jpn.*, 60, 3515.
- [17] Pongali Sathya Prabu, N., Vijayakumar, V. N., & Madhu Mohan, M. L. N. (2011). *Mol. Cryst. Liq. Cryst.*, 548, 73.
- [18] Vijayakumar, V. N., & Madhu Mohan, M. L. N. (2009). *Braz. J. Phy.*, 39(4), 677.
- [19] Pongali Sathya Prabu, N., Vijayakumar, V. N., & Madhu Mohan, M. L. N. (2011). *Mol. Cryst. Liq. Cryst.*, 548, 142.
- [20] Pongali Sathya Prabu, N., Vijayakumar, V. N., & Madhu Mohan, M. L. N. (2011). *Physica B*, 406, 1106.
- [21] Pongali Sathya Prabu, N., Vijayakumar, V. N., & Madhu Mohan, M. L. N. (2011). *Phase Transitions*, 1. In press.
- [22] Pongali Sathya Prabu, N., Vijayakumar, V. N., & Madhu Mohan, M. L. N. (2011). *Phase Transitions*, in press.
- [23] Vijayakumar, V. N., Murgugadass, K., & Madhu Mohan, M. L. N. (2010). *Mol. Cryst. Liq. Cryst.*, 517, 43.
- [24] Chitravel, T., & Madhu Mohan, M. L. N. (2010). *Mol. Cryst. Liq. Cryst.*, 524, 131.
- [25] Vijayakumar, V. N., & Madhu Mohan, M. L. N. (2010). *Mol. Cryst. Liq. Cryst.*, 517, 113.
- [26] Vijayakumar, V. N., & Madhu Mohan, M. L. N. (2009). *J. Opto. Elec. Adv.Mat.*, 11(8), 1139.
- [27] Vijayakumar, V. N., & Madhu Mohan, M. L. N. (2009). *Sol. State. Sci.*, 4, 482.
- [28] Vijayakumar, V. N., & Madhu Mohan, M. L. N. (2009). *Sol. State. Comm.*, 149, 2090.
- [29] Lehn, J. M. (1995). *Concept and Perspectives*, VCH: Weinheim; *Supramol. Chem.*.
- [30] Fouquey, C., Lehn, J. M., & Mlevelut, A. (1990). *Adv. Mater.*, 2, 254.
- [31] Pongali Sathya Prabu, N., Vijayakumar, V. N., & Madhu mohan, M. L. N. (2011). *J. Mol. Str.*, 994, 387.
- [32] Gray, G. W., & Goodby, J. W. G. (1984). *Smectic Liquid Crystals: Textures and Structures*, Leonard Hill: London.
- [33] Kato, T., Uryu, T., Kaneuchi, F., Jin, C., & Frechet, J. M. J. (1993). *Liq. Cryst.*, 14, 1311.
- [34] Pavia, D. L., Lampman, G. M., & Kriz, G. S. (2007). *Introduction to Spectroscopy*, Kundli: Sanat Printers.
- [35] Nakamoto, K. (1978). *Infrared and Raman Spectra of Inorganic and Co-Ordination Compounds*, Interscience: New York.
- [36] Xu, J. (2006). *J. Mater. Chem.*, 16, 3540.
- [37] Frechet, J. M. J., & Kato, T. (1992). Patent US No. 5,139,696.
- [38] Srinivasulu, M., Satyanarayana, P. V. V., Kumar, P. A., & Pisipati, V. G. K. M. (2002). *Z. Naturforsch.*, 56a, 685.
- [39] Noot, C., Perkins, S. P., & Coles, H. J. (2000). *Ferroelectrics*, 244, 331.
- [40] Chandrasekhar, S. (1977). *Liquid Crystals*, Cambridge University Press: New York.

- [41] Barmatov, E. B., Bobrovsky, A., Barmatova, M. V., & Shibaev, V. P. (1999). *Liq. Cryst.*, 26, 581.
- [42] Stanley, H. E. (1971). *Introduction to Phase Transition and Critical Phenomena*, Clarendon Press: New York.
- [43] Vijayakumar, V. N., & Madhu Mohan, M. L. N. (2009). *Ferroelectrics*, 392, 81.
- [44] Vijayakumar, V. N., & Madhu Mohan, M. L. N. (2010). *Z. Naturforsch.*, 65a, 1156.
- [45] Vijayakumar, V. N., & Madhu Mohan, M. L. N. (2010). *Physica B*, 405, 4418.
- [46] Adams, J. E. (1972). Patent US No. 3,679,290.
- [47] Adams, J. E. (1973). Patent US No. 3, 711, 181.
- [48] Goldberg, P., Hansford, J., & Van Heerden, P. J. (1971). *J. Appl. Phys.*, 42(10), 3874.